Assessing the effectiveness of streambank stabilization projects on the Cottonwood River using Unmanned Aircraft Systems

by Anthony L. Layzell and Alan Peterson

KGS Open-File Report 2020-16

INTRODUCTION

Reservoir sedimentation is a significant issue for Kansas, with three of the 24 federal reservoirs in the state expected to become more than 50% infilled by 2030 and another eight by the turn of the century (deNoyelles and Kastens, 2016). These projections have important implications for the sustainability of water supplies, flood protection, and aquatic habitats. Reducing sediment yields into reservoirs is a current priority in the Regional Advisory Committee Action Plans articulated in the Kansas Water Vision. For example, in the Neosho River watershed, reducing sedimentation rates into John Redmond Reservoir by an average of 300 acre-ft per year has been set as the first priority goal. The recognition that streambank erosion contributes a significant portion to total watershed sediment yield has resulted in the implementation of numerous streambank stabilization (SBS) projects along rivers draining into major federal reservoirs. For example, along the Cottonwood River, a tributary of the Neosho River, 23 SBS projects have been constructed to date and the current Neosho Regional Advisory Committee Action Plan proposes to stabilize all streambank hotspots, as defined by the Kansas Water Office (KWO), in the Neosho watershed above John Redmond Reservoir by 2025. The effectiveness of such SBS projects in reducing sediment yields, however, is currently unknown and therefore needs to be studied to determine whether SBS accomplishes the goal of reducing total sediment loads entering Kansas reservoirs. Determining SBS effectiveness can only be answered by long-term repeat monitoring. One of the major problems in determining SBS effectiveness, however, is the cost (e.g., time and money) of such monitoring. The use of Unmanned Aircraft Systems (UAS), however, provides a means to overcome these limitations and could prove to be a valuable tool for repeat monitoring of all SBS sites in Kansas.

Small UAS have emerged in recent years as effective remote sensing tools due to their low risk and economical cost (Carbonneau and Dietrich, 2017; Cook, 2017). UAS technology offers an effective means to collect very high-resolution imagery (cm scale or higher) that has wide-ranging application, including mapping geomorphic changes and quantifying streambank erosion in fluvial settings. Collected aerial images can be mosaicked together and georeferenced to generate local orthorectified aerial maps, known as orthomosaics, as well as digital elevation models (DEMs) using specialized image processing software. State-of-art photogrammetry techniques, such as structure from motion (SFM) and multiview stereo algorithms, are used in these software packages for picture alignment and positional error minimization. The horizontal and vertical accuracy of

products derived from UAS imagery have been shown to be comparable to similar products derived from LiDAR (Fonstad et al., 2013). This accuracy requires the use of either a Real Time Kinematic (RTK) Global Navigation Satellite System (GNSS) receiver onboard the UAS or the use of ground control points (GCPs). High-resolution UAS imagery has been used in many environmental applications, including riparian mapping (Jensen et al., 2011), bathymetry mapping (Lejot et al., 2007), channel topography characterization (Tamminga et al., 2015a; Woodget et al., 2015), and geomorphic change, including streambank erosion (Hamshaw et al., 2019; Tamminga et al., 2015b).

The overall objective of this project was to test the utility of UAS for assessing the effectiveness of SBS projects along the Cottonwood River. Specific goals included quantifying streambank erosion processes and estimating volumes of sediment eroded at 14 select SBS sites over time, including comparisons between (1) pre-construction and post-construction periods and (2) SBS sites and unmodified sites.

PROCEDURES

To quantify streambank erosion processes and assess the effectiveness of SBS projects, a total of 11 stream reaches along the Cottonwood River (Figure 1) were surveyed using UAS during spring 2019 with repeat surveys occurring during winter 2019. Reaches surveyed varied in length between 750 and 2,500 m and included (1) proposed SBS construction sites C102 and C112; (2) 14 constructed sites (C2, C3, C4, C5, C7, C9, C10, C11, C12, C13, C14, C15, C18, C62); and (3) six unmodified sites (U1–U6). Initial flight testing was performed at sites N16 and Nat 27 (Figure 1B).

Flight surveys were performed with a DJI Phantom 4 Pro platform equipped with a 20-megapixel camera. Flight surveys consisted of pre-programmed flight plans designed to collect imagery at nadir from altitudes of 60–118 m above the ground surface with 90% and 60% front and side overlap, respectively. Pre-programmed flight plans were supplemented with manual flight surveys designed to collect oblique imagery of the streambanks, particularly under overhanging vegetation. Manual missions were flown at altitudes of 30–70 m with camera angles oriented 5–30° from vertical. Between 500 and 899 images were collected per surveyed reach.

For georeferencing, between six and nine GCPs were installed for each reach. GCPs consisted of monumented rebar pins overlaid with colored 16x16 inch square plastic pavers. GCP positional information was obtained with a TopCon HiPer V RTK GNSS base and receiver. The HiPer V base station was installed over one GCP per reach and positional data collected every 15 seconds for at least two hours. The resulting data were corrected by the U.S. National Geodetic Survey Online Positioning User Service (OPUS). Positional data for remaining GCPs were collected with

the HiPer V receiver and were subsequently adjusted based on the OPUS-corrected coordinates for the base station.

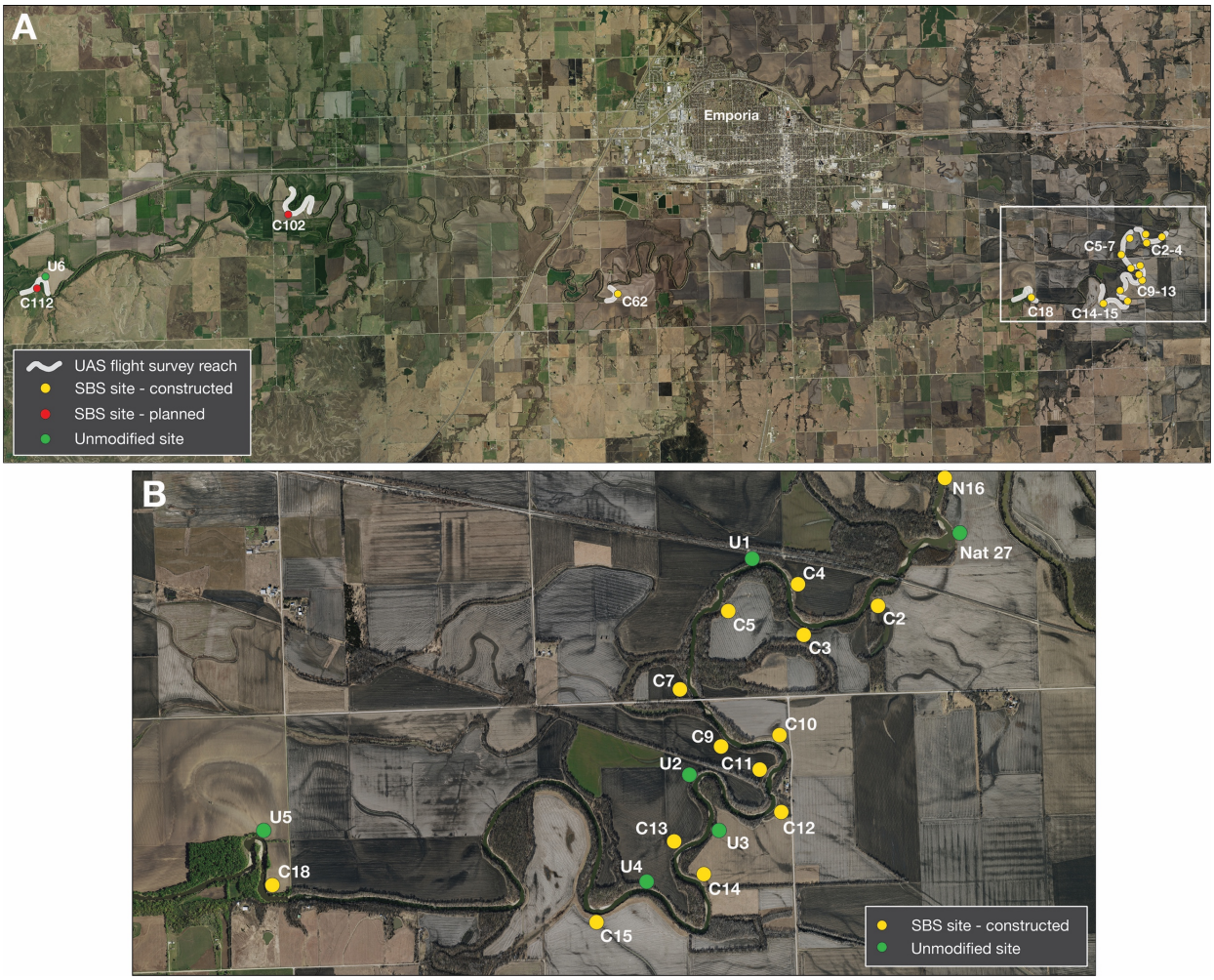

Figure 1. Location of study area. Images of UAS flight survey reaches and streambank stabilization sites are shown. Area in white box shown in B.

UAS images were processed to generate seamless orthomosaics and DEMs for each reach using Agisoft Photoscan Pro version 1.3.2 and Metashape Pro version 1.6.3. The workflow consisted of adding and aligning images, manually identifying and adjusting GCP locations, building a dense cloud, classifying ground points, and building a DEM from the ground points within the dense cloud. Final DEMs and orthoimagery were exported as tiff files for use in ESRI ArcMap (version 10.7) to assess the effectiveness of SBS projects.

The calculation of volumes of material eroded at each SBS site involved three phases:

Phase 1. Volumes eroded prior to SBS construction

Volumes of sediment eroded before SBS construction were determined from historical aerial imagery, i.e., Digital Orthophoto Quadrangles (DOQ) (1992, 2002), National Agriculture Imagery Program (NAIP) (2006, 2008, 2012), LiDAR (2010), and Kansas Next Generation 911 (NG911) (2014), following the Kansas Water Office procedure for conducting streambank assessments (KWO, 2017). All historical imagery was obtained from the Kansas Data Access and Support Center (DASC) at the Kansas Geological Survey with the exception of 1992 DOQ imagery, which was obtained from the USGS EarthExplorer. Imagery for each site was overlain in ArcMap and polygons were manually digitized based on observed changes in the location of the top of the streambank between images. The area of each polygon was then multiplied by the bank height to obtain an estimated volume of material eroded between each set of images. Bank height was calculated from LiDAR imagery based on the average of at least three measurements for each site.

Phase 2. Volumes eroded between construction and year 1 UAS flight survey

A common approach for quantifying geomorphic change involves the comparison of DEMs from successive surveys. By subtracting later DEMs from earlier DEMs, DEMs of Difference (DoDs) can be created to show volumetric changes over time. Given that constructed SBS sites were installed in the project area before flight survey monitoring began (i.e., between 2014 and 2017), a method was developed to create DEMs at the time of SBS construction based on As-Built total station survey data provided by The Watershed Institute, Inc. As-Built surveys were conducted immediately after SBS construction and included at least two control points per site. These control points were located, resurveyed with the TopCon HiPer V system, and used as GCPs during UAS flight surveys. As-Built survey point data were imported into ArcMap and adjusted using the "Adjust xy" tool to match control points common to both the As-Built survey and the UAS flight surveys. A Triangulated Irregular Network (TIN) model was created from the As-Built data and then converted into a DEM using the "TIN to raster" tool (Figure 2A). As-Built control points at sites C9, C10, and C11 were not able to be located and so As-Built DEMs were not generated at these sites. DoDs depicting the volumetric change at each site between the As-Built DEM and the first UAS flight survey DEM were generated using the "Cut Fill" tool (Figure 2B). Note that all DoDs were clipped to analyze the area of streambank between the water surface elevation and the top of the bank. This reduces error associated with water surface refraction and vegetation (see Tamminga et al., 2015a; Woodget et al., 2015).

Phase 3. Volumes eroded between UAS flight surveys

DEMs generated for each site from UAS flight surveys were imported into ESRI ArcMap. DoDs depicting the volumetric change between the first and second UAS flight survey DEMs were generated using the "Cut Fill" tool (Figure 2C).

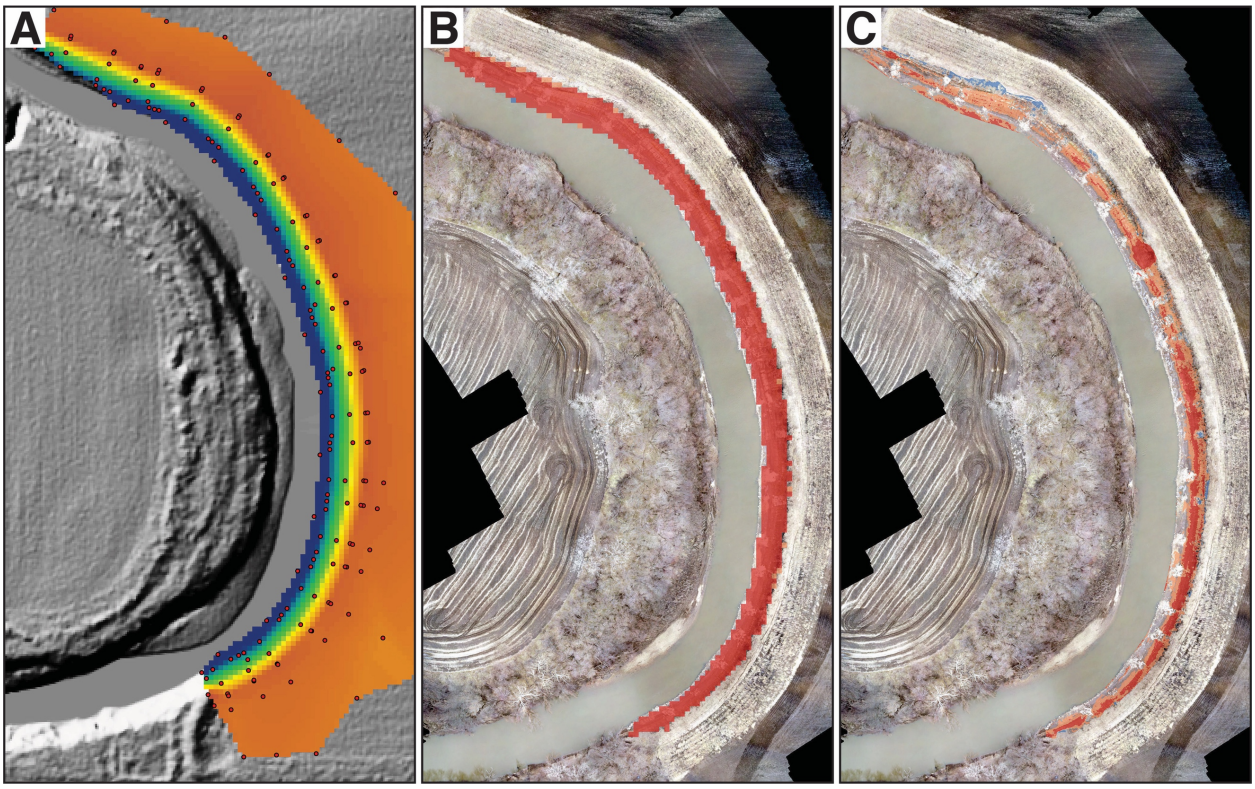

Figure 2. (A) Example of DEM created from As-Built total station survey point data (red circles) at site C62. Total station survey was performed on 4/7/15. Background imagery is 2010 LiDAR. (B) DoD image showing areas of material loss (red) and gain (blue) at site C62 between As-Built and first UAS flight survey (from 4/7/15 to 3/1/19). (C) DoD image showing areas of material loss (red) and gain (blue) at site C62 between first and second UAS flight surveys (from 3/1/19 to 10/16/19).

RESULTS AND DISCUSSION

Number and distribution of GCPs for streambank DEMs

UAS flight surveys were conducted on 5/7/18 at site N16 to test the number of GCPs needed to generate an accurate DEM of the streambank. GCPs were installed at both the top and bottom of the streambank (Figure 3A). Three DEMs of the streambank were generated using different numbers of GCPs: Model 1 using all 11 GCPs; Model 2 using three GCPs located at the top of the streambank; and Model 3 using only two GCPs located at the top of the streambank. DoDs were constructed by subtracting Models 2 and 3, respectively, from Model 1 in ArcGIS (Figure 3B and C). Results show that the difference in elevation between using all 11 GCPs and using three GCPs was predominantly less than 1 cm (Figure 3B). Based on the DEM generated from three GCPs, the remaining eight GCPs were used as checkpoints. The mean positional errors (x,y,z) of the remaining eight GCPs were calculated to be 0.02, 0.013, and 0.004 m.

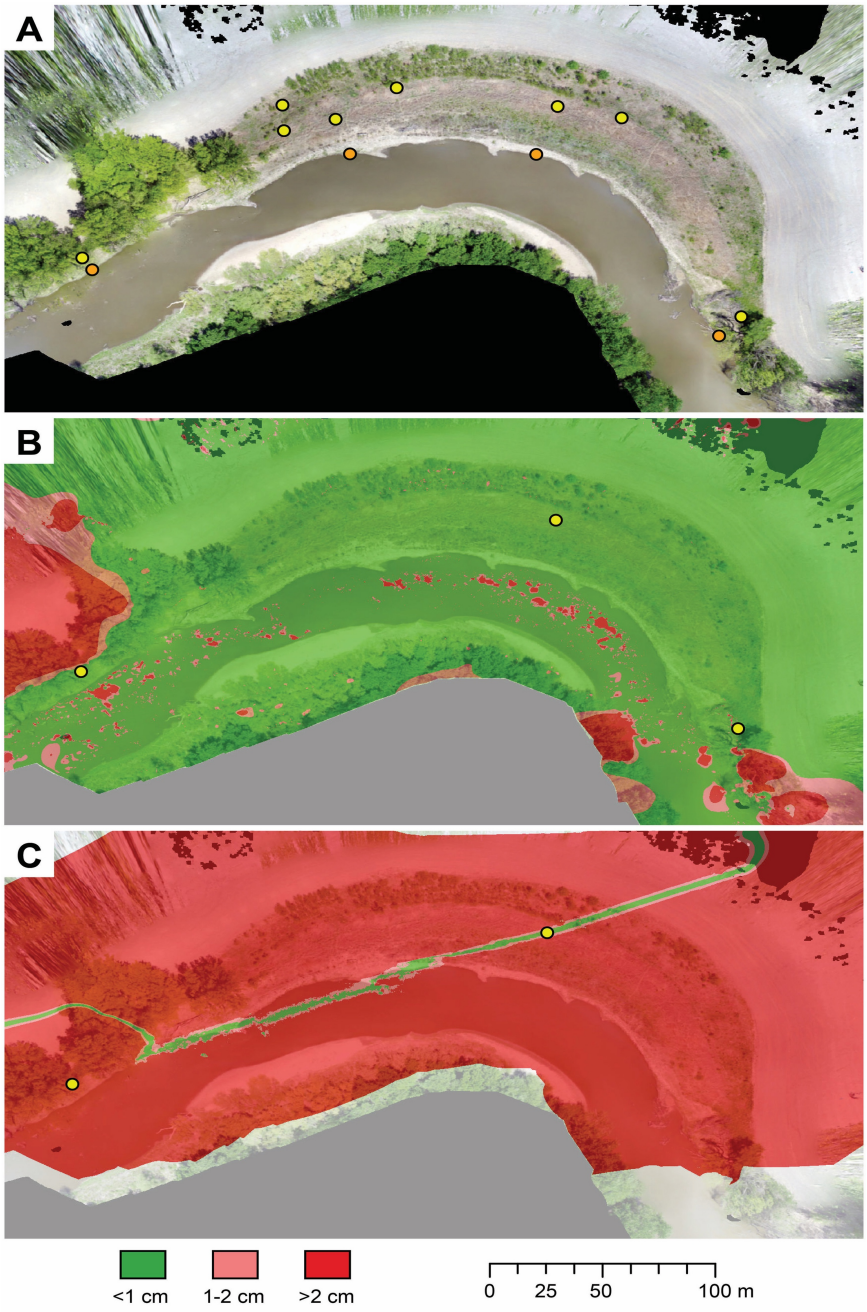

Figure 3. (A) Orthoimage of site N16 showing locations of GCPs installed at the top (yellow circles) and bottom (orange circles) of the streambank. (B) DoD showing difference between using all 11 GCPs and using 3 GCPs (Model 1-Model 2). (C) DoD showing difference between using all 11 GCPs and using 2 GCPs (Model 1-Model 3).

The main sources of error in the DEMs are associated with areas under tree canopy cover and areas of high refractivity associated with the water in the river channel (Figure 3B). Errors in the DEM generated using only two GCPs result from the inability to establish a plane in three dimensions and the subsequent increase in rotational error away from the axis between the two GCPs. This

observation has important implications for the spatial distribution of any number of GCPs, namely, that they must not be colinear.

UAS monitoring of flood events

In October 2018, the Cottonwood and Neosho rivers experienced out-of-bank flood discharges (Figure 5A). Daily mean discharges at the USGS Neosho Rapids gaging station (#07182390) ranged between 20,700 and 28,200 cfs October 9–12. Post-flood UAS flight surveys were conducted at site Nat 27 on November 1 and compared to a pre-flood flight survey flown on August 9. Figure 5B illustrates the DEM overlain with the orthomosaicked imagery generated from the post-flood flight.

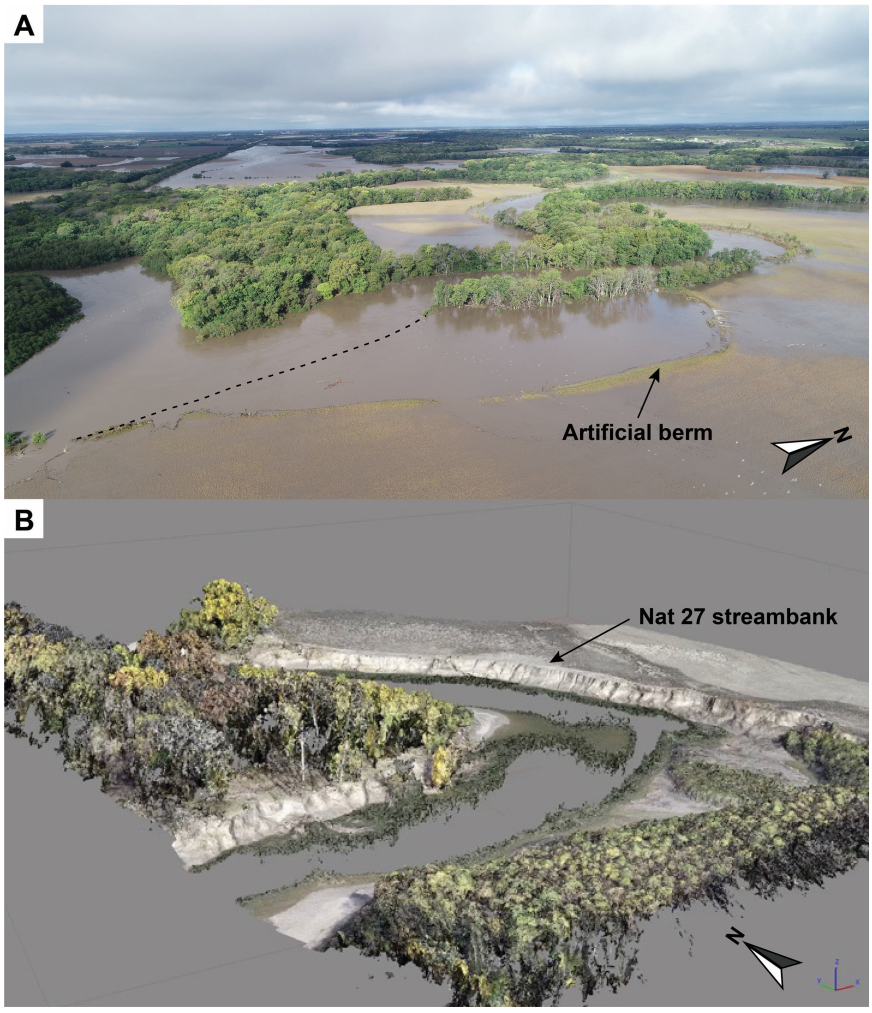

Figure 5. (A) UAS photograph of flooding immediately downstream of the Cottonwood-Neosho River confluence, October 10, 2018. Dotted line is the approximate location of the streambank at site Nat 27. (B) 3-D model of the streambank at site Nat 27 generated from a post-flood UAS flight survey flown on November 1, 2018.

Figure 6 shows the DoD generated from the pre- and post-flood UAS flight surveys. This analysis indicates that ~19,000 ft^3 of material was eroded from the right streambank at site Nat 27 during the October flood event. It was also determined, however, that ~37,800 ft^3 of material was deposited on the opposite point bar, resulting in a net gain of ~18,000 ft^3 of sediment at the site. It is important to note that the type of material deposited on the point bar is predominantly coarser-grained sediment (i.e., sand and gravel) and, therefore, not the fine-grained material typically associated with reservoir sedimentation. Future documentation of the mobility and stability of point bar features, however, is important as they may serve as locations of temporary storage for fine-grained sediment once stabilized and vegetated.

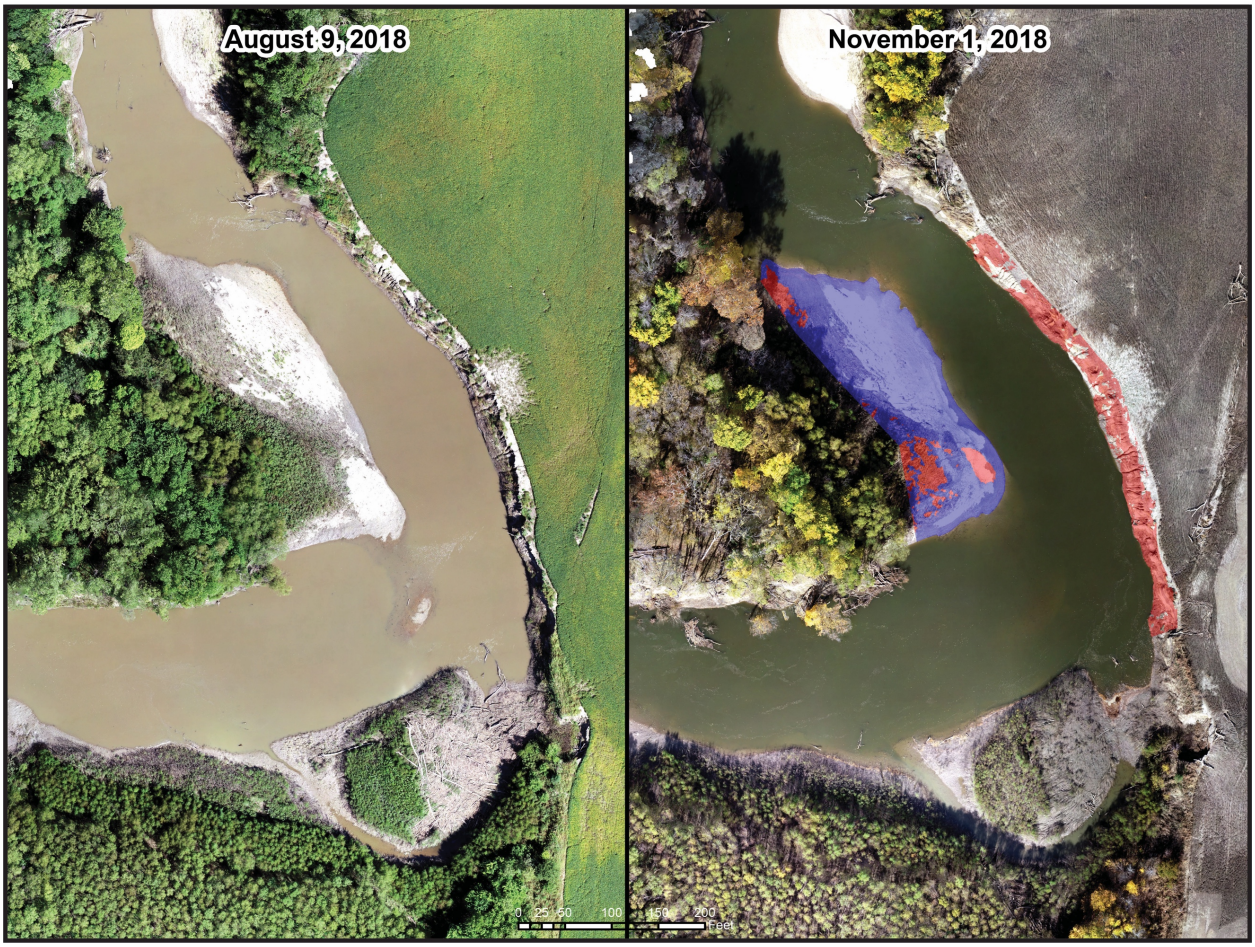

Figure 6. Orthomosaic images generated from pre-flood (left) and post-flood (right) UAS flight surveys. Red shading on post-flood image shows areas of loss/erosion and purple shading shows areas of gain/deposition calculated from DoD.

In addition to documenting the volume of material eroded from the streambank at site Nat 27, assessing the spatial patterns of bank erosion is informative. For example, erosion of the streambank from the October flood at site Nat 27 was not uniform. Localized areas of higher erosion were observed and were associated with rotational slumps. The largest slump feature at

site Nat 27 measured ~58 ft across at water level (Figure 7A). Comparison of pre- and post-flood UAS-derived DEMs indicates that ~4,700 ft^3 of material was associated with this rotational slump. In other words, this one slump feature represents 25% of the total volume eroded from the streambank but spatially represents ~12% of the total streambank area assessed. Slumping of streambanks usually occurs as flood stages recede due to (1) either undercutting or steeping of the bank by hydraulic erosion, (2) the loss of confining pressure, and (3) an increase in the weight of bank material due to saturation. Multiple rotational failures were observed at proposed construction site C102 after a flood event in March 2019 (Figure 7B). The propensity of streambanks to slump is a function of their geotechnical characteristics, including cohesion, matric suction, and internal friction angle (Simon et al., 2000). Ongoing geotechnical analyses of streambank material in the Cottonwood watershed seeks to investigate the susceptibility of streambanks to mass wasting (i.e., slumping) processes.

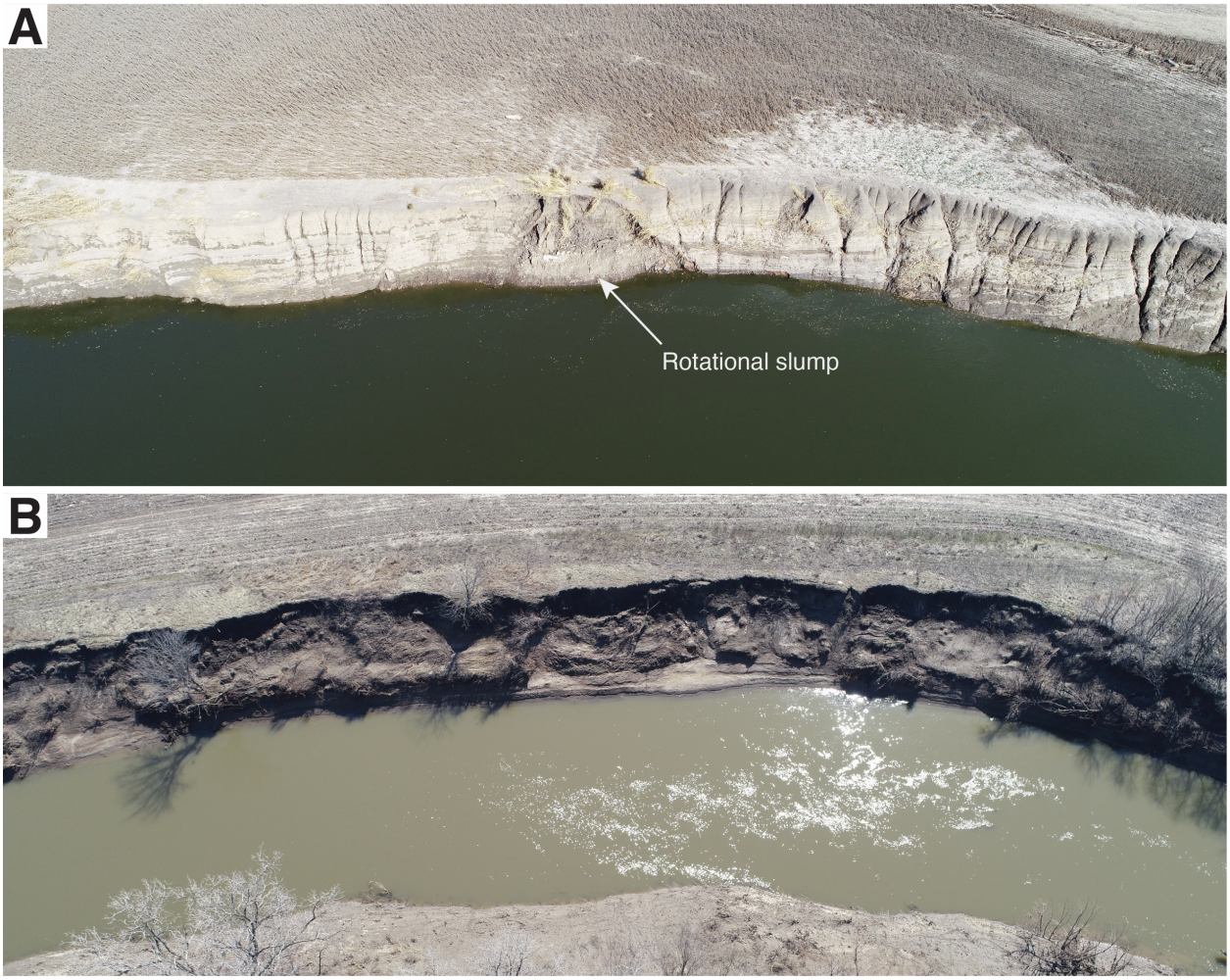

Figure 7. (A) Image of streambank at site Nat 27 showing rotational slump feature after flood event October 9–12, 2018. Image was taken on 11/1/2018. (B) Series of bank failures at proposed construction site C102 after a flood event March 13–15, 2019. Flood peaked at 9,620 cfs, which corresponds to a flood stage of about 25 ft. Image was taken on 3/21/19.

Assessing streambank stabilization effectiveness

As previously noted, a variety of different datasets were used to determine volumes of sediment eroded at each SBS site over time. In particular, pre-construction volumes were determined from assessment of historical aerial imagery, whereas post-construction volumes were determined from the generation of DoDs based on DEMs derived from As-Built and UAS flight survey data. Figure 8 shows the calculated volumes eroded at each site over time.

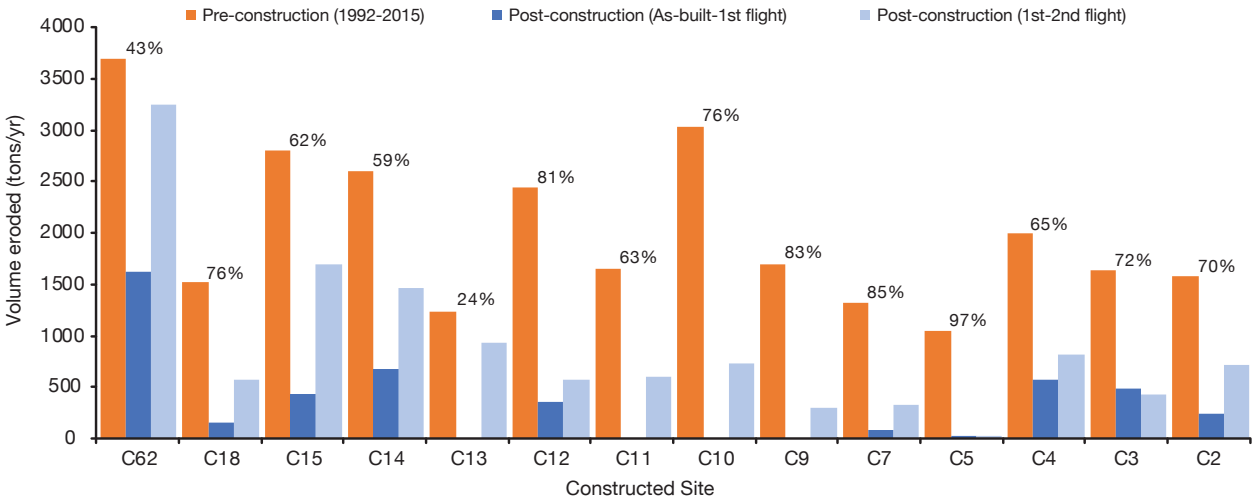

Figure 8. Pre- and post-construction volume of sediment eroded annually (tons/yr) at each SBS site. Percent efficiency in terms of sediment reduction is also shown for each site. Note that percent efficiency is based upon the average post-construction volume eroded per year (i.e., As-Built to second flight survey, where As-Built data were available).

Results indicate that streambanks have continued to erode after construction at every SBS site. The volume of material eroded per year was typically higher between the two UAS flight surveys compared to the volume calculated between the As-Built and first flight surveys. This observation can be attributed to differences in stream discharge between the two survey periods. For example, mean daily discharge per year on the Cottonwood River ranged from 123–786 cfs between 2014 and 2018 compared to 2,411 cfs in 2019 (USGS stream gage #07182250).

Importantly, post-construction erosion volumes are significantly less at each site compared to pre-construction values, indicating that SBS projects have significantly reduced erosion locally at each SBS site. Calculated percent efficiencies in reducing erosion, based upon the *average* post-construction volume eroded per year (As-Built to second flight) relative to the *average* pre-construction volume eroded per year (1992–2015), range from 24% to 97%. Using average values to calculate pre-construction volumes eroded per year, however, is less than ideal as significant variability was observed at each site between sets of historical aerial imagery (Figure 9).

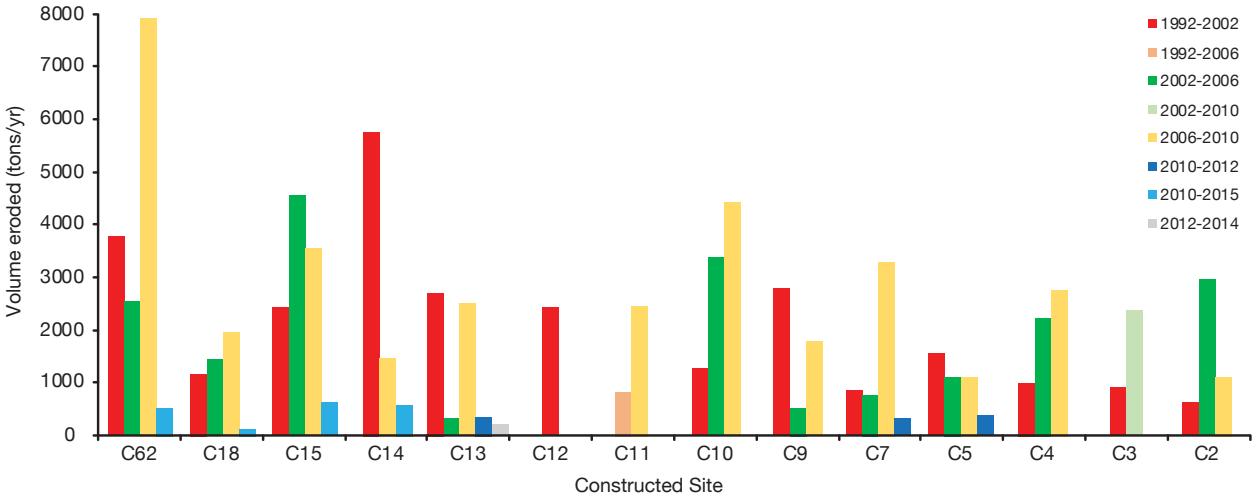

Figure 9. Average pre-construction volume of sediment eroded annually (tons/yr) at each SBS site between different sets of historical aerial imagery.

Using site C62 as an example, the volume of sediment eroded between the periods 2006–2010 and 2010–2015 is significantly different (i.e., more than 7,000 tons/yr; see Figure 9 and Table 1). This variability may be due in part to inaccuracies in the historical aerial imagery. For example, DOQ and NAIP imagery (1992–2012) was taken during leaf-on conditions, making it difficult to delineate the top of the streambank at some sites. Also, some historical imagery appeared to be inaccurately georeferenced. For example, a displacement of 1.53 m was measured for a road culvert near site C62 in subsequent sets of historical imagery (2012 NAIP and 2014 NG911) (Figure 10).

Figure 10. Image showing displacement of a fixed object (road culvert) between subsequent sets of historical imagery. Background image is 2014 NG911.

Where such displacement of fixed objects was observed, the inaccurate historical imagery was not used for the determination of pre-construction volumes of material eroded. Although all historical imagery was assessed for georeferencing inaccuracies, the lack of fixed objects in the study area means that the inclusion of such errors cannot be completely ruled out.

It is also important to note that each period analyzed differs hydrologically (i.e., in terms of the magnitude and frequency of flood events). Therefore, to account for these differences, total volumes eroded were normalized for the total volume of water (i.e., stream discharge) in a given period. Also, given that each SBS site is different in terms of the length of streambank stabilized, volumes eroded were normalized for length to facilitate comparison between individual sites (see Figures 11 and 12). The final equation used to determine normalized erosion values is:

$$N = (V / (Q \times L)) \times 1000 \quad (1)$$

Where N = normalized erosion, V = total volume eroded (ft^3), Q = total discharge (cfs), L = streambank length (ft). Total stream discharge for each period was calculated, using USGS gaging station data (Cottonwood River near Plymouth #07182250). Total discharge values were scaled for each site according to contributing drainage area.

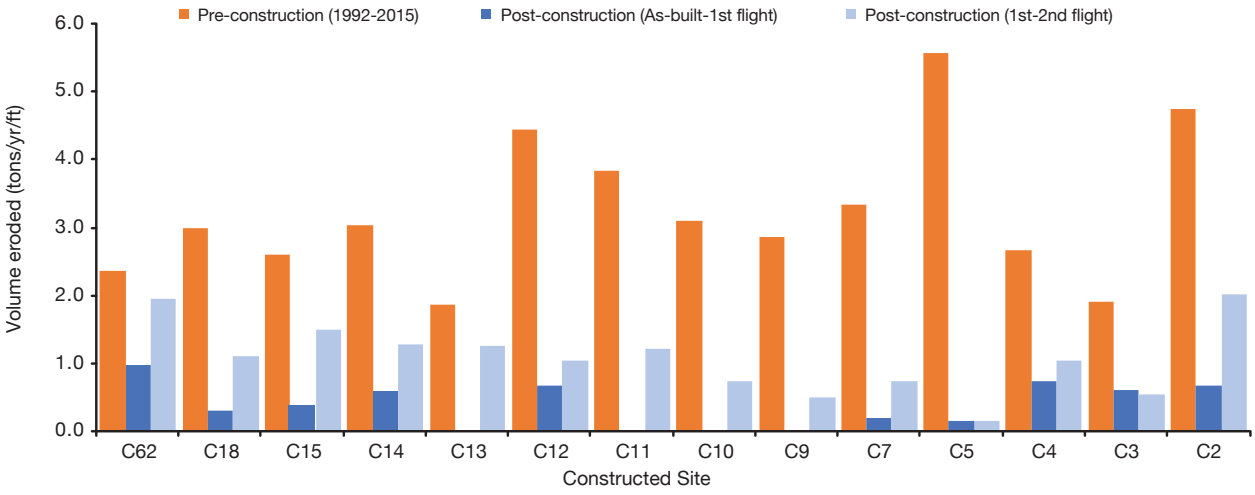

Figure 11. Average pre- and post-construction volume of sediment eroded annually per foot of streambank (tons/yr/ft) at each site.

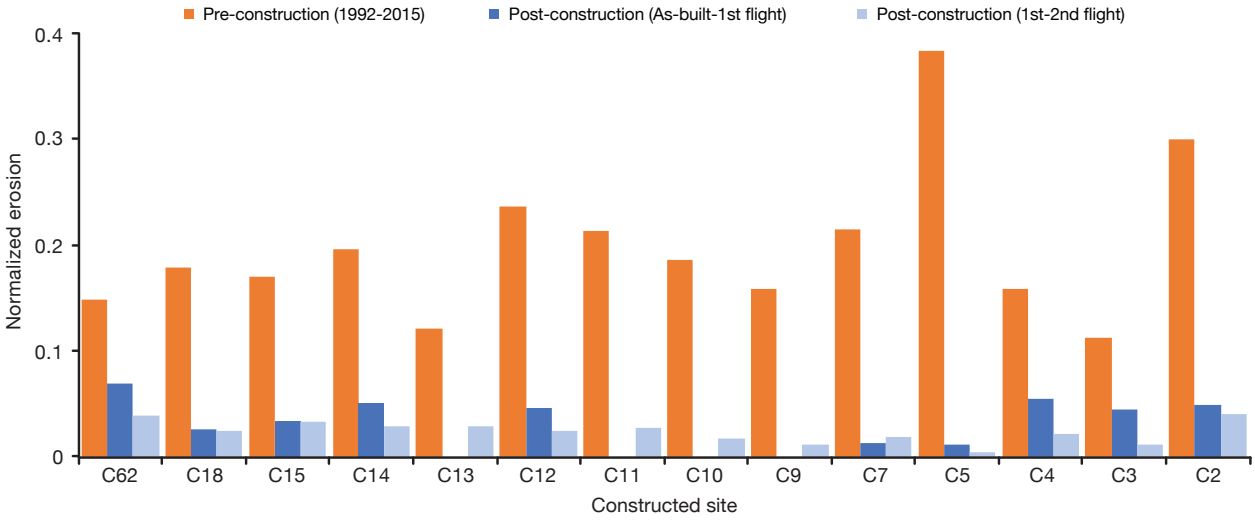

Figure 12. Average pre- and post-construction volume of sediment eroded normalized for length and total stream discharge.

Normalized data continue to show that SBS projects have significantly reduced erosion locally at each site. When normalized for both length and stream discharge, post-construction volumes of material eroded between the first and second UAS flight survey are typically less than volumes between the As-Built and the first UAS flight survey. This observation may result from the relatively coarse resolution of the DEM generated from As-Built point data compared to the cm scale resolution of the UAS-derived DEMs.

Table 1. Pre-construction (2006–2015) and post-construction (2015–2019) volumes of material eroded at site C62.

Site C62			Volume eroded				
Time period	No. days	No. years	Total (ft^3)	per year (ft^3/yr)	per year (tons/yr)	per year/bank length (tons/yr/ft)	Normalized erosion*
7/7/06–12/15/10	1,622	4.4	**790,978**	177,994	7,921	5.0	0.29
12/15/10–4/7/15	1,562	4.3	**50,959**	11,908	530	0.3	0.05
4/7/15–3/1/19	1,424	3.9	**142,142**	36,434	1,621	1.0	0.07
3/1/19–10/16/19	229	0.6	**45,838**	73,061	3,251	1.9	0.04

* Erosion values normalized according to equation 1.

Determination of SBS efficiency is highly dependent on the pre-construction period chosen for comparison. For example, at site C62, if the period 2010–2015 is used as the pre-construction baseline, then the SBS project can be deemed to be ineffective as post-construction volumes eroded are either comparable or greater, even when normalized for length and total discharge (Table 1). In contrast, if 2006–2010 data are used as the pre-construction baseline, then the SBS project can be considered to be effective as post-construction volumes eroded are significantly lower. Overall, these observations highlight the need for accurate and representative baseline data to compare to UAS-derived post-construction volumes eroded.

Because inaccuracies were observed in some of the historical aerial imagery, volumes of sediment eroded between UAS flight surveys were also calculated at eight unmodified reaches, including two proposed SBS sites (C102 and C112) for comparison (Figure 13). Results indicate that erosion at SBS sites was significantly less compared to the majority of unmodified sites. These results further support the conclusion that SBS projects are effective in locally reducing erosion.

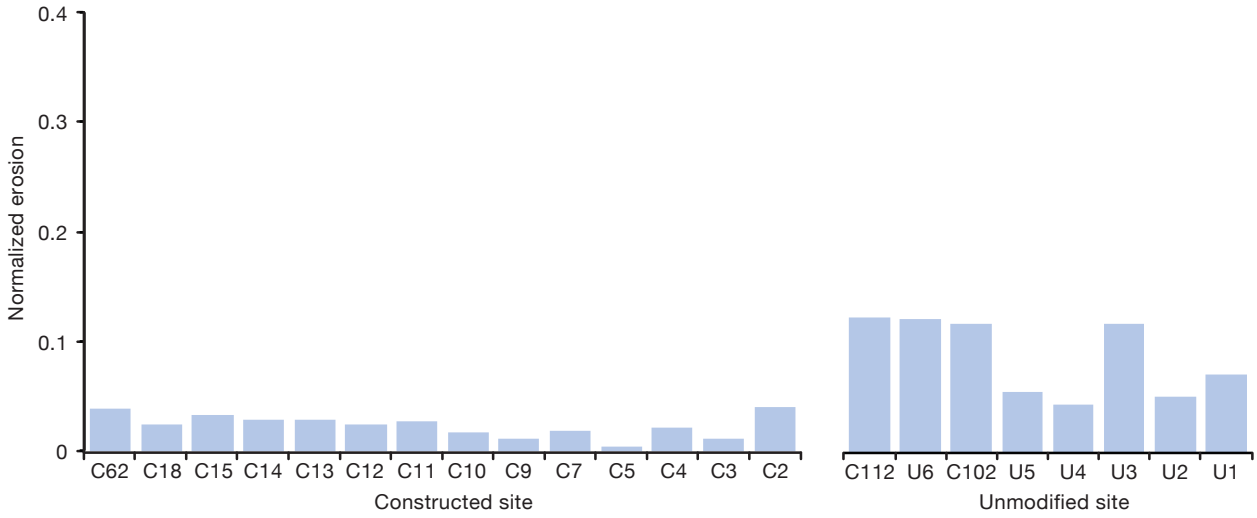

Figure 13. Post-construction volume of sediment eroded normalized for length and total stream discharge for SBS sites and unmodified sites between first and second flight surveys.

CONCLUSIONS

In sum, this study has shown that UAS technology can be used as a cost-effective means to (1) obtain high-resolution spatial data, (2) monitor geomorphic change, and (3) specifically assess the effectiveness of SBS projects. Results from two years of UAS monitoring, coupled with historical pre-construction assessment, indicate that SBS projects significantly reduce erosion locally at the stabilized site. Our assessment shows the importance of normalizing estimates of the volume of material eroded at each site (e.g., by time, streambank length, and stream discharge) to appropriately determine the effectiveness of SBS projects. However, quantification of sediment reduction and percent efficiency of SBS projects is only possible with accurate and representative baseline data. Pre-construction UAS monitoring, where possible, would provide a valuable baseline dataset. Such baseline data have been collected for proposed sites C102 and C112, which are currently scheduled to be constructed in the spring of 2021. Future work will focus on continued post-construction monitoring of SBS sites, with a strong emphasis on proposed sites C102 and C112. Also, there is significant variability in terms of efficiency between individual sites that warrants further investigation. Finally, potential upstream and downstream effects of SBS projects remain to be assessed to thoroughly evaluate SBS effectiveness.

ACKNOWLEDGMENTS

This project was funded by the Kansas Water Resources Institute (USGS 104(b) Water Resources Research grant 2018KS198B) and the Kansas Water Office. Special thanks to all the landowners who kindly provided access to streambank stabilization sites. The authors also thank Julie Tollefson for editorial comments.

REFERENCES

Carbonneau, P. E., & Dietrich, J. T. (2017). Cost-effective non-metric photogrammetry from consumer-grade sUAS: implications for direct georeferencing of structure from motion photogrammetry. *Earth Surface Processes and Landforms*, *42*(3), 473–486.

Cook, K. L. (2017). An evaluation of the effectiveness of low-cost UAVs and structure from motion for geomorphic change detection. *Geomorphology*, *278*, 195–208.

deNoyelles, F., & Kastens, J. H. (2016). Reservoir sedimentation challenges Kansas. *Transactions of the Kansas Academy of Science*, *119*(1), 69–81.

Fonstad, M. A., Dietrich, J. T., Courville, B. C., Jensen, J. L., & Carbonneau, P. E. (2013). Topographic structure from motion: a new development in photogrammetric measurement. *Earth Surface Processes and Landforms*, *38*(4), 421–430.

Hamshaw, S. D., Engel, T., Rizzo, D. M., O'Neil-Dunne, J., & Dewoolkar, M. M. (2019). Application of unmanned aircraft system (UAS) for monitoring bank erosion along river corridors. *Geomatics, Natural Hazards and Risk*, *10*(1), 1285–1305.

Jensen, A. M., Hardy, T., McKee, M., & Chen, Y. (2011). Using a multispectral autonomous unmanned aerial remote sensing platform (AggieAir) for riparian and wetlands applications. In *Geoscience and Remote Sensing Symposium (IGARSS), 2011 IEEE International* (pp. 3413-3416).

KWO (2017). John Redmond watershed streambank erosion assessment. Report prepared by the Kansas Water Office, March 2017.

Lejot, J., Delacourt, C., Piégay, H., Fournier, T., Trémélo, M. L., & Allemand, P. (2007). Very high spatial resolution imagery for channel bathymetry and topography from an unmanned mapping controlled platform. *Earth Surface Processes and Landforms*, *32*(11), 1705–1725.

Simon, A., Curini, A., Darby, S. E., & Langendoen, E. J. (2000). Bank and near-bank processes in an incised channel. *Geomorphology*, *35*(3-4), 193-217.

Tamminga, A., Hugenholtz, C., Eaton, B., & Lapointe, M. (2015a). Hyperspatial remote sensing of channel reach morphology and hydraulic fish habitat using an unmanned aerial vehicle (UAV): a first assessment in the context of river research and management. *River Research and Applications*, *31*(3), 379–391.

Tamminga, A. D., Eaton, B. C., & Hugenholtz, C. H. (2015b). UAS-based remote sensing of fluvial change following an extreme flood event. *Earth Surface Processes and Landforms*, *40*(11), 1464–1476.

Woodget, A. S., Carbonneau, P. E., Visser, F., & Maddock, I. P. (2015). Quantifying submerged fluvial topography using hyperspatial resolution UAS imagery and structure from motion photogrammetry. *Earth Surface Processes and Landforms*, *40*(1), 47–64.